

Czech Technical University in Prague
Faculty of Nuclear Sciences and Physical Engineering

HABILITATION LECTURE

Quantum Graphs
with Preferred-Orientation Coupling

Kvantové grafy
s vazbou preferované orientace

RNDr. Jiří Lipovský, Ph.D.

Summary

We study the model of quantum graphs with preferred-orientation coupling and state the main results in this area. Quantum graphs describe the behaviour of a quantum particle on a network. The preferred-orientation coupling, introduced to describe the anomalous quantum Hall effect, is an example of the vertex condition which, unlike the most common conditions, violates the time-reversal invariance. Moreover, it has significantly different high-energy transport properties for the odd and even vertex degrees. For the odd vertex degrees, the transport through the vertex is possible only in small energy windows and the lattice spectrum is usually dominated by the gaps. On the other hand, the vertices with even degrees allow the particle to reflect or scatter with similar probabilities and the lattice spectrum is dominated by the spectral bands. We give the main properties of the coupling and review the results in various models using the preferred-orientation coupling.

Keywords

quantum graphs, preferred-orientation coupling, spectrum, vertex degree

Souhrn

Studujeme model kvantových grafů s vazbou preferované orientace a uvádíme hlavní výsledky v této oblasti. Kvantové grafy popisují chování kvantové částice na síti. Vazba preferované orientace, zavedená pro popis anomálního kvantového Hallova jevu, je příkladem podmínky ve vrcholu, která, narozdíl od většiny běžných podmínek, porušuje symetrii na otočení času. Dále má zásadně odlišné transportní vlastnosti pro vysoké energie pro lichý a sudý stupeň vrcholu. Pro vrcholy lichého stupně se částice může přes vrchol přenést jen v úzkých energetických oknech a ve spektru mřížek většinou dominují mezery. Na druhou stranu vrcholy se sudým stupněm umožňují částici se odrazit nebo projít s podobnými pravděpodobnostmi a mřížka je dominována spektrálními pásy. Uvedeme hlavní vlastnosti této vazby a shrneme výsledky v různých modelech využívajících vazbu preferované orientace.

Klíčová slova

kvantové grafy, vazba preferované orientace, spektrum, stupeň vrcholu

Contents

1	Introduction	4
2	Description of the Model	5
3	Examples of the Coupling Conditions	6
4	Preferred-Orientation Coupling	8
5	Applications of the Preferred-Orientation Coupling	9
5.1	Square and Hexagonal Lattices	9
5.2	Platonic Solid Graphs	10
5.3	Bulk-Edge Effects	13
5.4	Other Results	16
6	Conclusion	16
	References	19
	RNDr. Jiří Lipovský, Ph.D. – CV	21

1 Introduction

The behaviour of a quantum particle on a network can be described by the model of quantum graphs. It joins the advantages of a rather simple model (from a mathematical point of view, it is a set of one-dimensional ordinary differential equations) and the complexity of the network, allowing the description of complicated phenomena.

The model has been popular since the 1980s, but its beginnings can be traced back to the 1930s in the work of L. Pauling [Pau36], who tried to describe the diamagnetic properties of aromatic molecules, or to the 1950s when K. Ruedenberg and C.W. Scherr [RS53] used it for the description of the electron behaviour in aromatic molecules.

The quantum graphs are a simplification of the model of *quantum wires* – a network model created from narrow structures allowing for a few transverse modes. In quantum graphs, the limit of the wire width going to zero is assumed. In the obtained one-dimensional structure only a single mode is assumed. However, various applications in mesoscopic physics are possible, for instance, for the description of nanowires or crystals (more details can be found e.g. in the monograph [BK13]). There are several generalizations of quantum graphs, for instance, *quantum waveguides* [EK15] or the networks build from quantum waveguides, so-called *fattened graphs* [Pos12]. From the mathematical point of view, both models are PDEs. Other generalizations are *hedgehog manifolds* joining a two- or three-dimensional Riemannian manifold with one-dimensional leads (see, e.g. [BEG03, EL13]) or *leaky graphs*, which allow for tunneling through the edges of the graph [Exn07].

For the behaviour of the quantum particle and the spectral properties of the model, not only the action of the operator on the graph's edges is important, but we must consider also the interaction at the vertices, the so-called coupling conditions. In the coupling conditions which are usually used (see Section 3), the time reversal invariance is fulfilled. However, the set of all possible self-adjoint coupling conditions is rich and allows for the operators to break the time reversal invariance. The aim of this text is to introduce one of them, named preferred-orientation coupling. As described in more detail in Section 4, for one particular value of energy, the wave incoming to the vertex “chooses” one particular direction and it is fully transmitted to the neighbouring edge. As explained in further sections, due to the presence or absence of the Dirichlet part of the coupling, the preferred-orientation coupling has substantially different transport properties in the cases when the vertex degree is odd or even. This results in different spectral properties.

The text is structured as follows. First, we introduce the model of quantum graphs in Section 2. Then we list the most common examples of coupling conditions (Section 3) and we focus on the preferred-orientation coupling (Section 4). In Section 5, we describe some of the results in the papers, where the preferred-orientation coupling was applied. Finally, we summarize its main properties (Section 6).

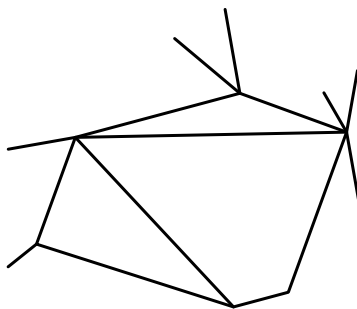


Figure 1: Example of a metric graph.

2 Description of the Model

Quantum graphs are, from a mathematical point of view, a set of ordinary differential equations. We assume a metric graph Γ which consists of a set of vertices \mathcal{V} and a set of edges \mathcal{E} . Usually, the set of edges consists of the set of N *internal edges* $\mathcal{E}_I = \{e_j\}_{j=1}^N$ of finite lengths $\ell_j > 0$ and the set of M *external edges* $\mathcal{E}_E = \{e_j\}_{j=N+1}^{N+M}$ of infinite lengths. The internal edges are parametrized by the intervals $(0, \ell_j)$ and their endpoints are vertices from the set \mathcal{V} . The external edges are parametrized by the intervals $(0, \infty)$ and represented by the half-lines with the endpoint being one of the vertices. The edges in the considered model are not oriented. We allow for multiple edges between given two vertices and edges starting and ending at one vertex. In this text, we will restrict ourselves only to graphs with internal edges, although we stress that the number of edges may be in some applications infinite. The *degree* of a vertex $\mathcal{X}_j \in \mathcal{V}$ is the number of edges emanating from it and is denoted by d_j . An example of a metric graph is sketched in Figure 1.

The corresponding Hilbert space for a graph with internal edges is

$$\mathcal{H} = \bigoplus_{i=1}^N L^2((0, \ell_i)).$$

We can represent the states in this Hilbert space by the vectors

$$\psi = (\psi_1, \dots, \psi_N)^T,$$

where ψ_j , $j = 1, \dots, N$ are the edge components of the wavefunction.

The whole structure is equipped with a second-order differential operator H acting as

$$H = -\frac{d^2}{dx^2} + q_j(x),$$

where $q_j(x)$ are the edge components of the (electric) potential depending on the coordinate on the edge, and $q_j(x)$ are bounded functions. However, in the next sections, the potential is assumed to be zero. This operator corresponds to the Hamiltonian of a quantum particle supported on the metric graph. For simplicity, we drop the factor $\frac{\hbar^2}{2m}$, usually appearing in the definition of the Hamiltonian in

quantum mechanics. This can be explained by considering a particular set of units, in which, e.g. the Planck constant $\hbar = 1$, and the mass $m = 1/2$.

In some applications, the particle is put into the magnetic field. Then the Hamiltonian acts as

$$H_A = - \left(\frac{d}{dx} - iA_j \right)^2 + q_j(x),$$

where A_j are the edge components of the magnetic potential.

The domain of the Hamiltonian consists of the functions in the Sobolev space $W^{2,2}(\Gamma)$ satisfying the coupling conditions. By this symbol we mean the orthogonal sum of the Sobolev spaces $W^{2,2}(e_j)$; we stress that the functions may not be continuous at the vertices. The general form of the coupling conditions (sometimes called matching or boundary conditions) at the vertex \mathcal{X}_j that define a self-adjoint operator is in the non-magnetic case

$$(U_j - I)\Psi_j + i(U_j + I)\Psi'_j = 0. \quad (1)$$

Here U_j is a $d_j \times d_j$ unitary matrix, I is the $d_j \times d_j$ identity matrix, i is the complex unit, Ψ_j is the $d_j \times 1$ column vector of the limits of function values from the edges to the vertex \mathcal{X}_j , and Ψ'_j is the $d_j \times 1$ column vector of the limits of outgoing derivatives at the vertex \mathcal{X}_j . We stress that the derivative must be taken in the outward direction, i.e. with the positive sign for $x = 0$ and the negative sign for $x = \ell_j$. The general form of the coupling conditions was obtained independently by V. Kostykin and R. Schrader [KS99] and M. Harmer [Har00].

Other formulations of the coupling conditions are possible. One can use square $d_j \times d_j$ matrices A_j and B_j instead of matrices $U - I$ and $i(U + I)$ in the equation (1); the conditions that make the operator self-adjoint are that the matrix $A_j B_j^*$ is self-adjoint (by the star we denote Hermitian conjugation here) and that, at the same time, the joint rectangular $d_j \times 2d_j$ matrix composed of matrices A_j and B_j has maximal rank. Another formulation uses the projectors to the Dirichlet part (the eigenspace of U corresponding to the eigenvalue -1), the projector to the Neumann part (the eigenspace of U corresponding to the eigenvalue 1) and Robin part (the complement of these two spaces) and gives the relation between them. Last we mention the formulation of the coupling conditions from [CET10]. It uses a particular form of the matrices A_j and B_j , where some of their blocks are zero. More details about these formulations of the coupling conditions and their comparison can be found, e.g., in [BK13, Lip16].

3 Examples of the Coupling Conditions

In this section, we list the most common coupling conditions which appear in quantum graphs and describe the coupling matrices corresponding to them.

1. Permutation Symmetric Coupling

The following class of coupling conditions with two complex parameters gives the coupling that is symmetric with respect to exchanging any two edges

adjacent to the vertex. The corresponding coupling matrix is $U = aJ + bI$, where I is the $d_j \times d_j$ identity matrix, J is the $d_j \times d_j$ matrix with all entries equal to one, and a and b are complex constants satisfying $|b|^2 = 1$, $|d_j a + b| = 1$ (these conditions insure unitarity of the matrix U).

2. δ -coupling

This coupling condition is a particular case of the permutation symmetric coupling. It is prescribed that the function values are continuous at the vertex while the sum of the outward derivatives is an α -multiple of the function value. Here, α is a real parameter which we will call the *coupling strength*. The condition at the vertex \mathcal{X} can be written as

$$\begin{aligned} f(\mathcal{X}) := f_i(\mathcal{X}) &= f_j(\mathcal{X}) \quad \text{for all } i, j \text{ such that } \mathcal{X} \in e_i \cap e_j, \\ \sum_{j: \mathcal{X} \in e_j} f'_j(\mathcal{X}) &= \alpha f(\mathcal{X}). \end{aligned}$$

If the vertex connects two edges, the condition corresponds to the interaction of the particle with the potential having the form of the δ -distribution. This gave the condition its name. The corresponding unitary coupling matrix is $U = \frac{2}{d_j + i\alpha} J - I$.

3. Standard Coupling

The standard coupling condition is a subcase of the δ -condition with $\alpha = 0$. The condition has various names; expressions such as ‘‘Kirchhoff’s’’, ‘‘free’’, ‘‘Neumann’’, ‘‘Kirchhoff-Neumann’’ are sometimes used. We stick to the name ‘‘standard’’, as it is the natural condition describing the free interaction of the particle at the vertex and it is very often used in papers. The name ‘‘Kirchhoff’s’’ is not fortunate, as the probability current conservation law is satisfied for all self-adjoint conditions. The condition can be written at the vertex \mathcal{X} as

$$\begin{aligned} f(\mathcal{X}) := f_i(\mathcal{X}) &= f_j(\mathcal{X}) \quad \text{for all } i, j \text{ such that } \mathcal{X} \in e_i \cap e_j, \\ \sum_{j: \mathcal{X} \in e_j} f'_j(\mathcal{X}) &= 0. \end{aligned}$$

The unitary coupling matrix is $U = \frac{2}{d_j} J - I$.

4. Dirichlet Coupling Conditions

If this coupling condition is prescribed at a vertex, the function values vanish at it. Therefore, the edges connected at the vertex do not interact with each other and they are fully decoupled. The condition can be written as

$$f_i(\mathcal{X}) = 0 \quad \text{for all } i \text{ such that } \mathcal{X} \in e_i.$$

The unitary matrix is $U = -I$.

5. Neumann Coupling Conditions

The vertex with the Neumann coupling condition is another example of a fully decoupled vertex. Unlike the Dirichlet condition, now the derivatives vanish at the vertex. The condition is

$$f'_i(\mathcal{X}) = 0 \quad \text{for all } i \text{ such that } \mathcal{X} \in e_i.$$

The unitary matrix is $U = I$. The reader should not be confused with the fact that some authors mean the standard coupling condition by this name.

4 Preferred-Orientation Coupling

We will devote the whole section to introducing the last coupling condition. In this text, we will pay attention to one particular coupling that appeared first in the paper [ET18]. The motivation of the authors of the mentioned paper was to describe the anomalous quantum Hall effect in the square and hexagonal lattices. This coupling does not belong to the class of permutation symmetric couplings. Moreover, it is an example of the coupling violating the time-reversal invariance.

The corresponding unitary coupling matrix has the form of a circulant matrix

$$U = \begin{pmatrix} 0 & 1 & 0 & \dots & 0 \\ 0 & 0 & 1 & \dots & 0 \\ \vdots & \vdots & \vdots & \ddots & \vdots \\ 0 & 0 & 0 & \dots & 1 \\ 1 & 0 & 0 & \dots & 0 \end{pmatrix}. \quad (2)$$

This form assures that for a particular value of energy $E = 1$ the wave arriving into the vertex from one edge is fully transmitted to the neighbouring edge (let's denote it by number 2); the incoming wave from the edge number 2 is fully transmitted to the edge number 3, etc. (see Figure 2).

However, the described behaviour does not hold for the general value of energy. For the high-energy limit, we can observe different behavior for odd and even degrees of the vertex. For odd vertex degrees, the scattering matrix for large energies converges to the scattering matrix for the fully decoupled case with Neumann coupling conditions. Hence it is difficult for the particle to transport through the vertex. On the other hand, for the even vertex degrees, the transport is quite easy; for instance, for degree four, there is asymptotically the same probability that the particle reflects to the same edge or transmits to any other adjacent edge. This difference between even and odd vertex degrees is caused by the properties of the eigenvalues of the coupling matrix U . In the even degree case, the eigenvalue -1 is present in the spectrum of U and hence the Dirichlet part of the coupling is present. This is not the case for the odd-degree vertices. From this, the asymptotic properties follow. The observation made in this paragraph was first obtained in [ET18], where the scattering matrices for vertex degrees 3 and 4 were obtained.

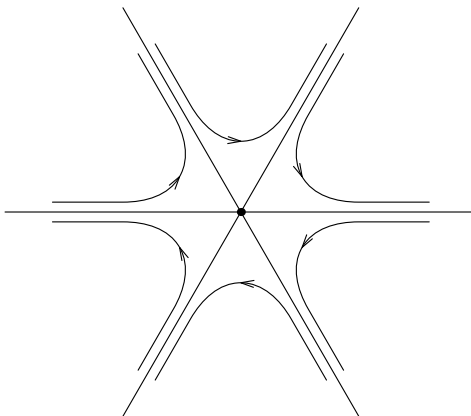


Figure 2: Illustration of waves transmitted through the vertex for the preferred-orientation coupling and the energy $E = 1$.

5 Applications of the Preferred-Orientation Coupling

5.1 Square and Hexagonal Lattices

The seminal paper [ET18] introduced quantum graphs with preferred-orientation coupling for the first time and studied their main properties. Inspired by the application of graphs to the anomalous quantum Hall effect in the paper [SK15], the authors tried to find the graphs that allow rotational motion in the lattice model but at the same time belong to the class of Hamiltonians with the self-adjoint coupling conditions given by eq. (1). They proposed the coupling given by the unitary matrix (2) and investigated the behaviour of the corresponding scattering matrix.

They found that the scattering matrix is

$$S(k) = \frac{1 + \eta}{1 + \eta + \eta^2} \begin{pmatrix} -\frac{\eta}{1+\eta} & 1 & \eta \\ \eta & -\frac{\eta}{1+\eta} & 1 \\ 1 & \eta & -\frac{\eta}{1+\eta} \end{pmatrix} \quad (3)$$

for the vertex degree three (hexagonal lattice) and

$$S(k) = \frac{1}{1 + \eta^2} \begin{pmatrix} -\eta & 1 & \eta & \eta^2 \\ \eta^2 & -\eta & 1 & \eta \\ \eta & \eta^2 & -\eta & 1 \\ 1 & \eta & \eta^2 & -\eta \end{pmatrix}$$

for the vertex degree four (square lattice), where $\eta = \frac{1-k}{1+k}$ with k being the momentum ($E = k^2$). The form (3) implies that the scattering matrix $S(k)$ converges to the identity matrix in the limit $k \rightarrow \infty$ ($\eta \rightarrow -1$).

Moreover, the authors also described the spectra of the square and hexagonal lattices with the preferred-orientation coupling. Let ℓ be the edge length for both

lattices. One of their results is that for the square lattice, there are infinitely many gaps in the absolutely continuous spectrum. They are asymptotically centered in the momentum variable k around $\frac{m\pi}{\ell}$, $m \in \mathbb{Z}$ and their width is approximately $\frac{4}{\pi m}$. Hence bands dominate the spectrum at high energies. In the energy variable, the gaps are asymptotically constant, since we have the following relation for the differentials $dE = 2k dk$. On the other hand, for the hexagonal lattice, the gaps asymptotically dominate the spectrum.

5.2 Platonic Solid Graphs

In the paper [EL19], symmetric equilateral (having edge lengths equal to one) graphs with finitely many edges were investigated. These graphs consist of vertices and edges of Platonic solids. All five Platonic solids were considered: tetrahedron, cube, octahedron, dodecahedron, and icosahedron. The corresponding very symmetric graphs appear as shapes of several molecules which can lead to the possible applications of this research. For instance, the methane has the shape of the tetrahedron, cubane of the cube, SF_6 of the octahedron, dodecahedrane of the dodecahedron, or boron of the icosahedron.

In [EL19] two types of coupling conditions were considered: the δ -conditions at all vertices and the preferred-orientation coupling with the same orientation if seen from the outside of the solid. The main interest of the paper was to find the asymptotic positions of the graphs' eigenvalues. Since the δ -condition is not the main topic of this text, we limit ourselves to stating that the main result of the paper is that the eigenvalues for δ -condition converge to those of the graphs with standard coupling.

However, the graphs with preferred-orientation coupling showed more interesting behaviour. One can observe that the only Platonic solid having an even degree of vertices is the octahedron (vertex degree 4), while the other Platonic solids have the odd degree of vertices (3 for the tetrahedron, the cube, and the dodecahedron and 5 for the icosahedron). Since the Platonic solids with the odd degree of vertices have the vertex scattering matrices converging to those of the decoupled Neumann conditions, one can expect that the Hamiltonians on the corresponding graphs will have eigenvalues converging to the eigenvalues of the Laplacian on the interval of length one with Neumann boundary conditions at both ends. The reason for this behaviour is that the graph for high energies effectively decouples to intervals of length one with Neumann boundary conditions. On the other hand, the octahedron has a different limiting vertex scattering matrix and the behaviour of the eigenvalues of the corresponding quantum graph may be different.

As we proved in [EL19], the behaviour of the eigenvalues is exactly as expected in the previous paragraph. For the four Platonic solid graphs with odd vertex degrees, the square root of the n -th eigenvalue is contained in the interval of the width of order $1/n$ centered around $n\pi$. As n grows to infinity, the width of the interval in the momentum scale shrinks and the square roots of eigenvalues approach multiples of π . However, we stress that this does not necessarily need to be the case for the energy variable. Since the differential of the energy is

$dE = 2k dk$ and k scales as n , the $\mathcal{O}(1/n)$ difference between the ends of the allowed interval in the momentum scale means that the distance of the eigenvalues in the energy scale from $n^2\pi^2$ is at most asymptotically constant. As an example of the eigenvalue behaviour for odd-degree graphs, we copy the statement of the theorem for the tetrahedron. For the cube, dodecahedron, and icosahedron, the theorem is very similar.

Theorem 5.1. *For the tetrahedron with the preferred-orientation coupling, the (square roots of) eigenvalues k are for large k contained in the intervals*

$$k_n \in \left(n\pi - \frac{2\sqrt{3}}{n\pi} + \mathcal{O}\left(\frac{1}{n^2}\right), n\pi + \frac{2\sqrt{3}}{n\pi} + \mathcal{O}\left(\frac{1}{n^2}\right) \right), \quad n \in \mathbb{Z}.$$

The behaviour of the octahedron graph is different. Since the probabilities of reflection and transmission to any adjacent edge are approximately the same, the graph in the high-energy limit does not decouple into separate intervals and there are other eigenvalues possible.

Theorem 5.2. *The (square roots of) eigenvalues for the octahedron with the preferred-orientation coupling are at $k = 2\pi n$ (with multiplicity eight) and $k = \pm\frac{2}{3}\pi + 2\pi n$ (with multiplicity two) with $n \in \mathbb{Z}$; the other (square roots of) eigenvalues are situated in the intervals*

$$k_n^{(1)} \in \left(\pi + 2\pi n - \frac{\sqrt{10}}{\pi + 2\pi n} + \mathcal{O}\left(\frac{1}{n^2}\right), \pi + 2\pi n + \frac{\sqrt{10}}{\pi + 2\pi n} + \mathcal{O}\left(\frac{1}{n^2}\right) \right),$$

$$k_n^{(2)} \in \left(\frac{\pi}{2} + \pi n - \frac{5}{(\frac{\pi}{2} + \pi n)^2} + \mathcal{O}\left(\frac{1}{n^4}\right), \frac{\pi}{2} + \pi n + \frac{5}{(\frac{\pi}{2} + \pi n)^2} + \mathcal{O}\left(\frac{1}{n^4}\right) \right).$$

Let us briefly comment on the proofs. To obtain the secular equation for finding the eigenvalues of the graph, one usually writes down the solution of the eigenvalue equation $-f''(x) = k^2 f(x)$ on the edges. Since the fundamental system of the given equation consists of the functions e^{ikx} and e^{-ikx} , the general solution on the j -th edge is $\tilde{a}_j e^{ikx} + \tilde{b}_j e^{-ikx}$ or, equivalently $a_j \sin(kx) + b_j \cos(kx)$. Then one substitutes these solutions into the coupling conditions at the vertices and arrives at $2N$ equations for $2N$ variables a_j, b_j . This system of equations can be written in the form

$$M(k)(a_1, b_1, \dots, a_N, b_N)^T = 0,$$

where $M(k)$ is a k -dependent $2N \times 2N$ matrix. The condition of solvability of the system is $\det M(k) = 0$, which is the secular equation for the eigenvalues of the Hamiltonian.

However, this standard approach is not very suitable for large graphs. Since the dodecahedron and icosahedron have 30 edges, computing the determinant of the 60×60 matrix would be time-consuming. Therefore, we used the quotient graph theory summarized in the paper by R. Band, G. Berkolaiko, C. H. Joyner, and W. Liu [BBJL17]. This allows for obtaining simpler, so-called quotient graphs

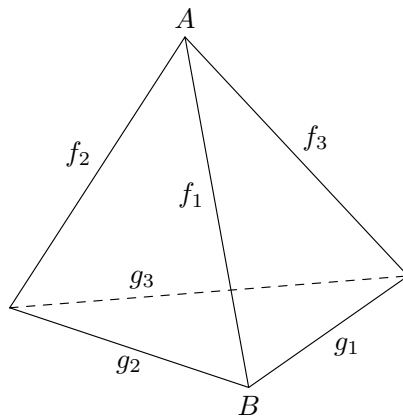


Figure 3: A tetrahedron. Reproduced from [EL19].

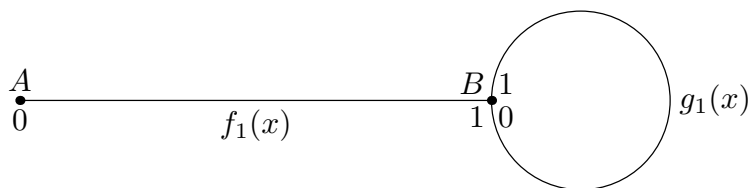


Figure 4: The quotient graph for the tetrahedron. Reproduced from [EL19].

with the domains corresponding to the eigenspaces of the operator of the symmetry. Decomposing the domain of the original Hamiltonian into the eigenspaces of the operator of the symmetry, one can find that the original Hamiltonian is unitarily equivalent to the orthogonal sum of the Hamiltonians on the quotient graphs. The secular equations for the quotient graphs can be obtained more easily.

In the paper [EL19], we did not use the whole symmetry of the graphs, but only the rotational symmetry of the Platonic solid graph. Let there be an n -fold symmetry axis of the graph and the operator of the rotation by $2\pi/n$ be T_n . Since the n -th power of this operator is the identity ($T_n^n = \text{id}$), its eigenvalues are $e^{\frac{2\pi i j}{n}}$ for $j = 0, \dots, n-1$. We decompose the domain of the original Hamiltonian into the eigenspaces of T_n and each eigenspace corresponds to a quotient graph. Then we obtain the secular equation for the eigenvalues as described in the previous paragraph. Finally, we obtain the first term of the high-energy asymptotics of the secular equation and get the asymptotic positions of the eigenvalues.

As an illustration of the process, we show the construction of the quotient graphs in the case of the tetrahedron. Let us denote the wavefunction components on the edges of the tetrahedron by $f_1, f_2, f_3, g_1, g_2, g_3$ as in Figure 3 and parametrize the edges by intervals $(0, 1)$ so that for $f_j, j = 1, 2, 3$, the point $x = 0$ is denoted by A . The point B corresponds to $x = 1$ for $f_1, x = 0$ for g_1 and $x = 1$ for g_2 . Moreover, we assume that the point $x = 0$ for g_3 corresponds to $x = 1$ for g_1 .

We define the operator T_3 as the rotation by $2\pi/3$ around the axis defined by the vertex A and the center of the opposite side. The rotation is assumed to be clockwise if seen from the outside of the tetrahedron. Denoting the eigenvalues of

T_3 by $\omega_j = e^{\frac{2\pi i}{3}j}$, $j = 0, 1, 2$, we assume subspaces where the following relations hold.

$$\begin{aligned} f_2(x) &= \omega_j f_1(x), & f_3(x) &= \omega_j^2 f_1(x), \\ g_2(x) &= \omega_j g_1(x), & g_3(x) &= \omega_j^2 g_1(x). \end{aligned} \quad (4)$$

Using the coupling condition (1) with the matrix (2) we have for the vertex A

$$\begin{pmatrix} -1 & 1 & 0 \\ 0 & -1 & 1 \\ 1 & 0 & -1 \end{pmatrix} \begin{pmatrix} f_1(0) \\ f_2(0) \\ f_3(0) \end{pmatrix} + i \begin{pmatrix} 1 & 1 & 0 \\ 0 & 1 & 1 \\ 1 & 0 & 1 \end{pmatrix} \begin{pmatrix} f'_1(0) \\ f'_2(0) \\ f'_3(0) \end{pmatrix} = 0.$$

After substituting from (4), the previous equation results for $j = 0$ in

$$-f_1(0) + f_1(0) + i(f'_1(0) + f'_1(0)) = 0, \quad \Rightarrow \quad f'_1(0) = 0.$$

and for $j = 1, 2$ in

$$-f_1(0) + \omega_j f_1(0) + i(f'_1(0) + \omega_j f'_1(0)) = 0, \quad \Rightarrow \quad f'_1(0) = (-1)^j \sqrt{3} f_1(0). \quad (5)$$

A slightly more complicated condition is obtained at the vertex B . Hence we for each j arrive at one quotient graph. Each of the three quotient graphs has the structure shown in Figure 4, but different coupling conditions at the vertices. E.g., at the vertex A there is the Neumann condition for the first graph and Robin condition (5) for the other two graphs.

5.3 Bulk-Edge Effects

In the publication [EL20], the quantum graphs with preferred-orientation coupling with an infinite number of edges were studied. There are two types of lattices suggested, and from each of them a straight strip is cut and the transport properties are investigated. Different vertex degrees near the edge of the strip and in the middle of the strip cause different high-energy transport properties.

The first lattice is *rectangular* (see Fig. 5a) and the vertex degrees at the edge of the strip are equal to three, while the vertex degrees in the bulk (at the internal vertices) are four. At all the vertices we assume preferred-orientation coupling. The lengths of the horizontal edges are ℓ_1 and the lengths of the vertical edges are ℓ_2 . As written in the previous sections, the odd-degree vertices are not “transport-friendly” at high energies, to be more precise, they allow the particle to transport only in a small window for the momentum k near the multiples of π/ℓ_2 . On the other hand, the transport in the bulk is quite easy, since there are even-degree vertices. The following theorem states that the generalized eigenfunction components at the edge of the strip are of order $\mathcal{O}(1/k)$.

Theorem 5.3. *Let us consider the rectangular lattice. For a fixed $K \in (0, \frac{1}{2}\pi)$, consider momenta $k > 0$ such that $k \notin \bigcup_{n \in \mathbb{N}_0} \left(\frac{n\pi - K}{\ell_2}, \frac{n\pi + K}{\ell_2} \right)$. Suppose that the restriction of the generalized eigenfunction corresponding to energy k^2 to the elementary cell is normalized, then its components at the leftmost and rightmost vertical edges are at most of order $\mathcal{O}(k^{-1})$.*

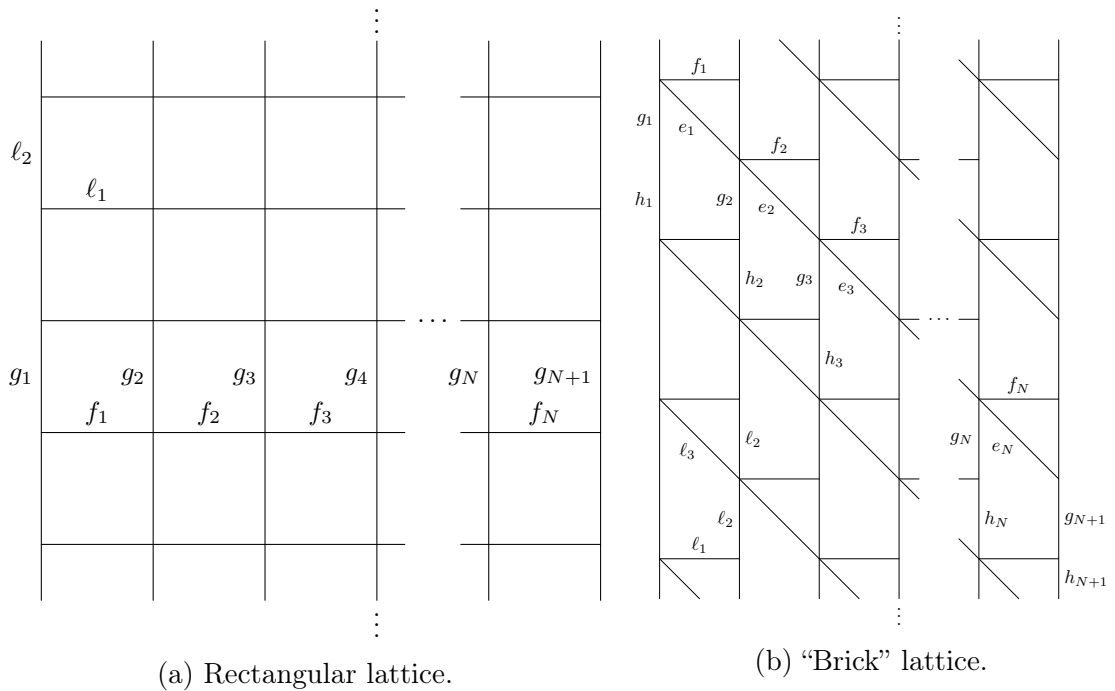


Figure 5: Rectangular (left) and “brick” (right) lattice strips. Reproduced from [EL20].

The second type of the lattice was named *brick* lattice since it somehow resembles the wall of bricks rotated by 90 degrees (see Fig. 5b). The edge lengths ℓ_1 , ℓ_2 , ℓ_3 are denoted in the figure. It is interesting that the vertex degrees are even (equal to four) only at the left edge of the strip. The vertices have odd degrees (three and five) in the bulk and at the right edge of the strip. Therefore, one expects that transport is possible only near the left edge of the strip. To make this statement more rigorous, we denote by $q_j^{(m)}$ the coefficients of the components of the generalized eigenfunctions in the j -th cell from the left. I.e. the leftmost cell has $j = 1$, the neighbouring $j = 2$, etc. The index m distinguishes the edge in the cell. The next theorem states that for momenta k that are far from the multiples of π/ℓ_i , the coefficients $q_j^{(m)}$ are of order $\mathcal{O}(k^{1-j})$. In other words, the generalized eigenfunctions decay as the distance from the leftmost edge increases.

Theorem 5.4. *Let us consider the “brick” lattice. For a fixed $K \in (0, \frac{1}{2}\pi)$, consider momenta $k > 0$ such that*

$$k \notin \bigcup_{n \in \mathbb{N}_0} \left(\frac{n\pi - K}{\ell_1}, \frac{n\pi + K}{\ell_1} \right) \cup \bigcup_{n \in \mathbb{N}_0} \left(\frac{n\pi - K}{\ell_2}, \frac{n\pi + K}{\ell_2} \right) \cup \bigcup_{n \in \mathbb{N}_0} \left(\frac{n\pi - K}{\ell_3}, \frac{n\pi + K}{\ell_3} \right). \quad (6)$$

Suppose again that the restriction of the generalized eigenfunction corresponding to energy k^2 to the elementary cell is normalized, then $q_j^{(m)}$ is at most of order $\mathcal{O}(k^{1-j})$ as $k \rightarrow \infty$.

Let us now briefly comment on the proofs. Their main essence is the Bloch-

Floquet decomposition. We sew the usual ansatzes (the combination of the exponentials e^{ikx} and e^{-ikx}) using the coupling conditions and the Bloch-Floquet parameter at the end of the cell. We use the fact that the scattering matrix at odd-degree vertices converges to the identity matrix for high energies. By comparison of the equations the claim follows.

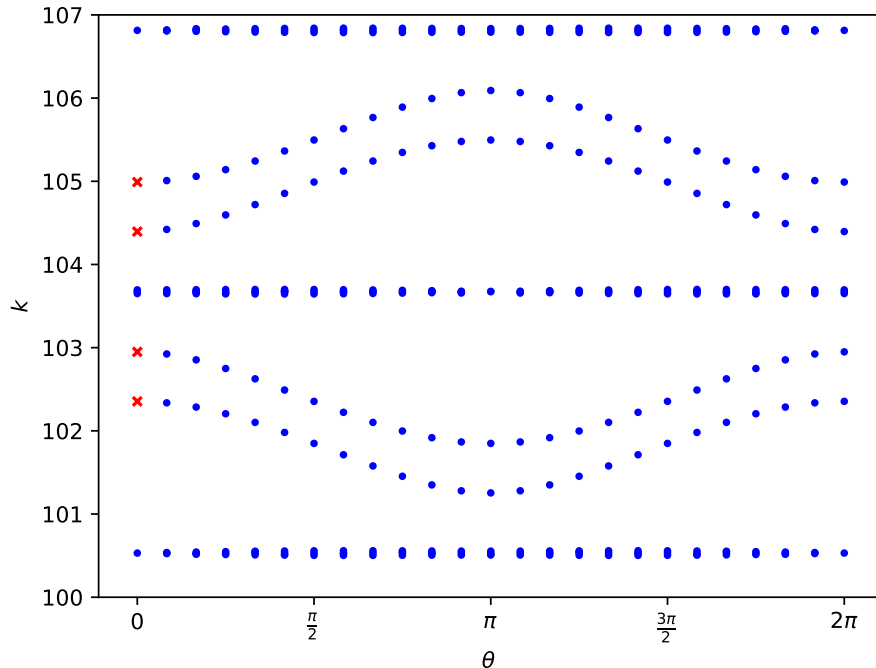


Figure 6: Dispersion diagram for the rectangular lattice strip, the points marked by red crosses are used in Figure 7. θ is the Bloch-Floquet parameter. Reproduced from [EL20].

The obtained theoretical results were supported also numerically. In this text, we show the numerical results for the rectangular lattice with three cells in the horizontal direction. The dispersion diagram (dependence of the momentum on the Bloch-Floquet parameter) was obtained for momenta k slightly larger than 100 (see Figure 6). For the points marked by the red crosses in Figure 6, the components of the generalized eigenfunction are shown in Figure 7. Let the coefficients by the exponentials for the edge components of the generalized eigenfunction be a_j and b_j for the vertical edges and c_j and d_j for the horizontal edges. In the left panel of Figure 7, there are the values of $||b_j|^2 - |a_j|^2|$ and $||d_j|^2 - |c_j|^2|$, proportional to the probability current, shown. There are four different values of k considered. The results for the four vertical edges are connected by lines (similarly to the three horizontal edges). One can see that the probability current on the leftmost and rightmost vertical edge is by three or four degrees of magnitude smaller than for the two vertical edges in the middle of the strip. This corresponds to the fact that the generalized eigenfunction components on the leftmost and rightmost edge are

of order $\mathcal{O}(1/k)$, the probability current is of order $\mathcal{O}(1/k^2)$ and $k \sim 100$. Similar results can be seen in the right panel of Figure 7 for the values of $|a_j|^2 + |b_j|^2$ and $|c_j|^2 + |d_j|^2$. Hence the numerical results correspond to the theoretical results.

5.4 Other Results

Let us now comment on the results in other papers. The paper [BET20] considered Laplacians on infinite tightly and loosely connected chains of rings (see Figures 8 and 9). The preferred-orientation coupling is assumed on both types of graphs. Using the result of [BLS19] one can prove that the spectrum of the Hamiltonian on the loosely connected ring chain converges to the spectrum of the Hamiltonian of the tightly connected ring chain if the length of the connecting edge goes to zero. As apparent from the figures, the tightly connected ring chain has vertex degree four, while the loosely connected one has vertex degree three. Similarly to [ET18], for the loosely connected rings, the gaps dominate the spectrum. On the other hand, for the tightly connected rings, the absolutely continuous part of the spectrum consists of the interval $[0, \infty)$.

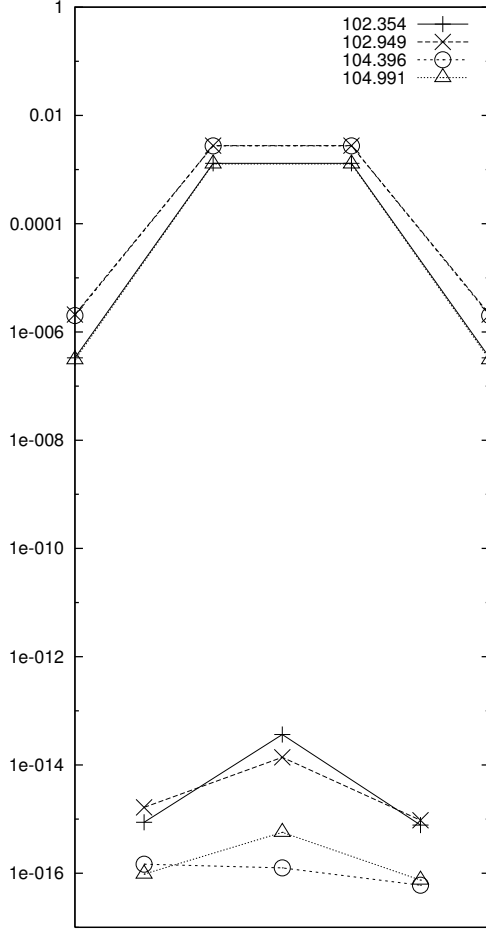
More general models were considered also in [BET22] and in [BEL22], where the connecting link between the cycles of the loosely connected chain does not necessarily have to be placed symmetrically (see Figure 10). In [BET22], the Hamiltonian acted as the negative second derivative and attention was paid to the structure of the bands and the probability that an arbitrary positive real number lies in the spectrum. Moreover, a theorem on the number of negative bands is given. In [BEL22], the magnetic Hamiltonian on a loosely connected ring chain and two types of tightly connected ring chains were considered. In one of the tightly connected ring chains, the edge of the length ℓ_1 is neglected, in the other, the limit $\ell_2 \rightarrow 0$ is considered. The properties of the positive and negative spectra are found and the probability that an arbitrary positive real number lies in the spectrum is researched. It was proven that the so-called Band-Berkolaiko universality [BB13] originally proposed for graphs with the standard coupling condition holds true also for the preferred-orientation coupling. The Band-Berkolaiko universality says that the above-mentioned probability does not depend on the edge lengths, as long as they are incommensurate.

In [BE22], the kagome and triangular lattices were considered. The spectra in these cases also consist of an infinite number of bands (some of them flat) and three (in the case of the kagome lattice) or two (in the case of the triangular lattice) negative bands. The Band-Berkolaiko universality is obtained here as well.

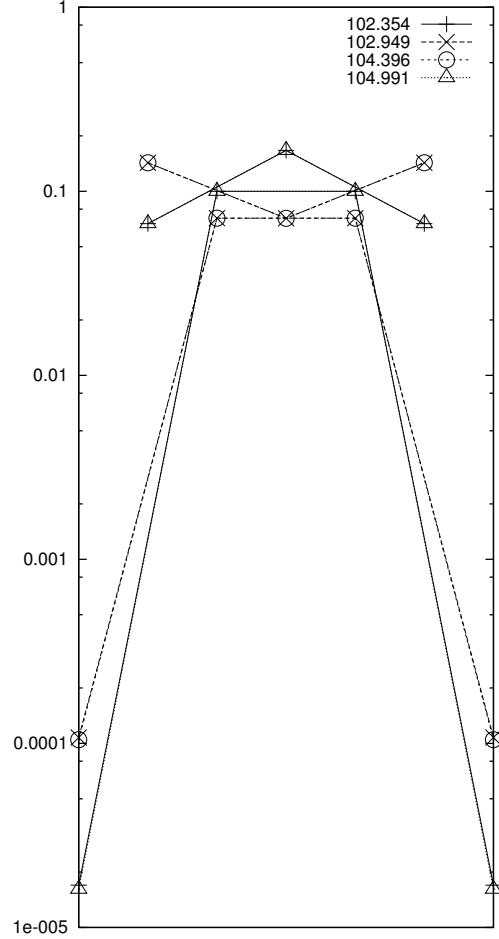
A brief review of some results on preferred-orientation coupling can be found in [Exn21]. A larger class of couplings with the coupling matrix being a circulant matrix is studied in [ET21]; attention is paid to the symmetry of the model.

6 Conclusion

We have introduced the class of quantum graphs with the coupling condition of preferred orientation. The Hamiltonian with this coupling condition serves as an



(a) Values of coefficients $||b_j|^2 - |a_j|^2|$ and $||d_j|^2 - |c_j|^2|$, proportional to probability current.



(b) Values of coefficients $|a_j|^2 + |b_j|^2$ and $|c_j|^2 + |d_j|^2$.

Figure 7: Rectangular lattice strip with 3 cells in the horizontal direction: values of two combinations of the coefficients a_j, b_j, c_j, d_j . For the particular values of k in the absolutely continuous spectrum shown in the caption (102.354, 102.949, 104.396, and 104.991) and $\theta = 0$ we plot the modulus of the difference $|b_j|^2 - |a_j|^2$ (or $|d_j|^2 - |c_j|^2$) proportional to the probability current (left panel) and the sum $|a_j|^2 + |b_j|^2$ (or $|c_j|^2 + |d_j|^2$) (right panel). The values are connected by lines indicating the value of k . The points are arranged according to the corresponding vertex positions in the strip, the three connected points correspond to the coefficients on the horizontal edges. Reproduced from [EL20].

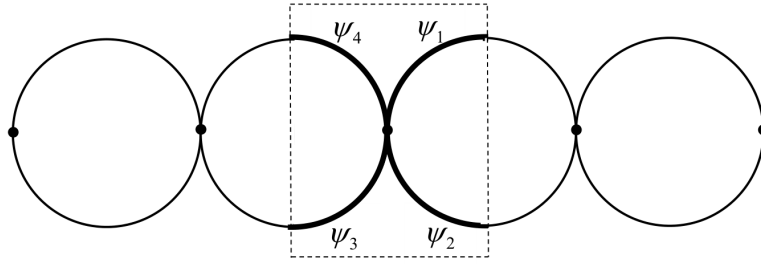


Figure 8: An elementary cell for the tightly connected ring chain. Reproduced from [BET20].

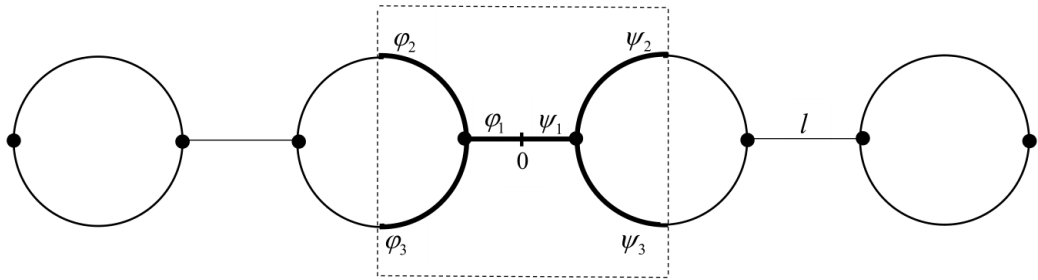


Figure 9: An elementary cell for the loosely connected ring chain. Reproduced from [BET20].

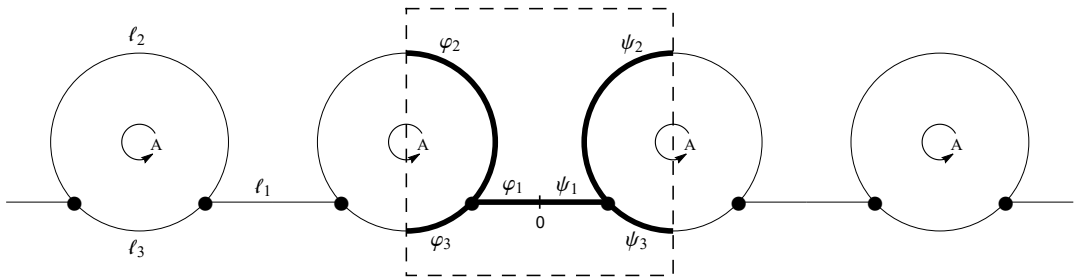


Figure 10: An elementary cell for the general loosely connected ring chain. Reproduced from [BEL22].

example of the operator violating the time-reversal invariance. Moreover, as the results show, there is a significant difference between the behaviour of such an operator if there are odd or even vertex degrees. For the odd vertex degrees, the transport through the vertex is difficult and hence for infinite graphs the gaps usually dominate the absolutely continuous spectrum. On the other hand, the transport through the vertices with an even degree is quite easy and typically the band-and-gap structure of the spectrum is dominated by the bands.

References

- [BB13] BAND, R. AND BERKOLAIKO, G. Universality of the momentum band density of periodic networks. *Phys. Rev. Lett.*, 2013. vol. 113, p. 130404.
- [BBJL17] BAND, R., BERKOLAIKO, G., JOYNER, C. H., AND LIU, W. Quotients of finite-dimensional operators by symmetry representations, 2017. ArXiv preprint, arXiv:1711.00918.
- [BE22] BARADARAN, M. AND EXNER, P. Kagome network with vertex coupling of a preferred orientation. *J. Math. Phys.*, 2022. vol. 63, p. 083502.
- [BEG03] BRÜNING, J., EXNER, P., AND GEYLER, V. A. Large gaps in point-coupled periodic systems of manifolds. *J. Phys. A: Math. Gen.*, 2003. vol. 36, no. 17, p. 4890.
- [BEL22] BARADARAN, M., EXNER, P., AND LIPOVSKÝ, J. Magnetic ring chains with vertex coupling of a preferred orientation. *J. Phys. A: Math. Theor.*, 2022. vol. 55, p. 375203.
- [BET20] BARADARAN, M., EXNER, P., AND TATER, M. Ring chains with vertex coupling of a preferred orientation. *Rev. Math. Phys.*, 2020. vol. 32, p. 2060005.
- [BET22] BARADARAN, M., EXNER, P., AND TATER, M. Spectrum of periodic chain graphs with time-reversal non-invariant vertex coupling. *Ann. Phys.*, 2022. vol. 443, p. 168992.
- [BK13] BERKOLAIKO, G. AND KUCHMENT, P. *Introduction to Quantum Graphs*, vol. 186 of *Mathematical Surveys and Monographs*. AMS, 2013. ISBN 978-0-8218-9211-4.
- [BLS19] BERKOLAIKO, G., LATUSHKIN, Y., AND SUKHTAIEV, S. Limits of quantum graph operators with shrinking edges. *Adv. Mat.*, 2019. vol. 352, pp. 632–669.
- [CET10] CHEON, T., EXNER, P., AND TUREK, O. Approximation of a general singular vertex coupling in quantum graphs. *Ann. Phys.*, 2010. vol. 325, pp. 548–578.

- [EK15] EXNER, P. AND KOVAŘÍK, H. *Quantum Waveguides*. Springer International, Heiderberg, 2015. ISBN 978-3-319-18575-0.
- [EL13] EXNER, P. AND LIPOVSKÝ, J. Resonances on hedgehog manifolds. *Acta Polytechnica*, 2013. vol. 53, pp. 416–426.
- [EL19] EXNER, P. AND LIPOVSKÝ, J. Spectral asymptotics of the Laplacian on Platonic solids graphs. *J. Math. Phys.*, 2019. vol. 60, p. 122101.
- [EL20] EXNER, P. AND LIPOVSKÝ, J. Topological bulk-edge effects in quantum graph transport. *Phys. Lett. A*, 2020. vol. 384, p. 126390.
- [ET18] EXNER, P. AND TATER, M. Quantum graphs with vertices of a preferred orientation. *Phys. Lett. A*, 2018. vol. 382, pp. 283–287.
- [ET21] EXNER, P. AND TATER, M. Quantum graphs: self-adjoint, and yet exhibiting a nontrivial \mathcal{PT} -symmetry. *Phys. Lett. A*, 2021. vol. 416, p. 127669.
- [Exn07] EXNER, P. Leaky quantum graphs: A review. In *Analysis on Graphs and Applications*, vol. 77 of *Proceedings of Symposia in Pure Mathematics*. 2007 pp. 523–564.
- [Exn21] EXNER, P. Quantum graphs with vertices violating the time reversal symmetry. *Physics of Elementary Particles and Atomic Nucleus*, 2021. vol. 52, pp. 330–336. In Russian, English translation.
- [Har00] HARMER, M. Hermitian symplectic geometry and extension theory. *J. Phys. A: Math. Gen.*, 2000. vol. 33, pp. 9193–9203.
- [KS99] KOSTRYKIN, V. AND SCHRADER, R. Kirchhoff’s rule for quantum wires. *J. Phys. A: Math. Gen.*, 1999. vol. 32, no. 4, pp. 595–630.
- [Lip16] LIPOVSKÝ, J. Quantum graphs and their resonance properties. *Acta Physica Slovaca*, 2016. vol. 66, no. 4, pp. 265–363.
- [Pau36] PAULING, L. The diamagnetic anisotropy of aromatic molecules. *J. Chem. Phys.*, 1936. vol. 4, pp. 673–677.
- [Pos12] POST, O. *Spectral Analysis on Graph-like Spaces*. Springer, Heidelberg, Heidelberg, 2012. ISBN 978-3-642-23839-0.
- [RS53] RUEDENBERG, K. AND SCHERR, C. Free-electron network model for conjugated systems, I. Theory. *J. Chem. Phys.*, 1953. vol. 21, pp. 1565–1581.
- [SK15] STŘEDA, P. AND KUČERA, J. Orbital momentum and topological phase transformation. *Phys. Rev. B*, 2015. vol. 92, p. 235152.

RNDr. Jiří Lipovský, Ph.D. – CV

Date of birth: February 29th, 1984
Email: jiri.lipovsky@uhk.cz
Webpage: <https://lide.uhk.cz/prf/ucitel/lipovji1/>
ORCID: <https://orcid.org/0000-0002-1845-1104>
Web of Science: <https://www.webofscience.com/wos/author/record/1197399>
Scopus: <https://www.scopus.com/authid/detail.uri?authorId=57219227487>

Education:

2014: Charles University in Prague, Faculty of Mathematics and Physics,
RNDr. degree: Physics, Theoretical Physics, Astronomy
2008 – 2011: Charles University in Prague, Faculty of Mathematics and Physics,
Ph.D. study programme: Physics, Theoretical Physics, Astronomy and
Astrophysics, (thesis title: Quantum graphs and their generalizations)
2006 – 2008: Charles University in Prague, Faculty of Mathematics and Physics,
master study programme: Physics, Theoretical Physics, summa cum laude
2003 – 2006: Charles University in Prague, Faculty of Mathematics and Physics,
bachelor study programme: Physics, General Physics, summa cum laude

Work experience:

2008 – 2012 and 2017 – 2019: Nuclear Physics Institute, Czech Academy of Sciences,
Ph.D. student and researcher
2012 – 2013: University of Lisbon, postdoctoral researcher
2012 to present: University of Hradec Králové, Faculty of Science, postdoc
and assistant professor
2018 – 2019: 6-month stay at the University of Lisbon

Publications

- 24 papers on WOS (8 in Q1, including 2 in D1)
- 159 citations including 110 citations without self-citations according to WOS
- h-index: 7 according to WOS, 8 according to Scopus
- publications e.g. in Phys. Rev. Lett., J. Diff. Eq., Phys. Rev. E, J. Funct. Anal.

Conferences

- invited speaker at six international conferences

- 23 presented talks at international conferences
- organizer of the international conference “Chaos, and what it can reveal – A conference on the occasion of Petr Šeba’s 60th birthday”, Hradec Králové, Czech Republic (May 2017) and national conference “11th meeting of Czech mathematical physicists”, Hradec Králové, Czech Republic (June 2018)

Reviews

- served as a reviewer for J. Phys. A: Math. Theor. (6x), J. Math. Phys. (2x), Anal. Math. Phys. (2x), Integral Equ. Oper. Theory, Nonlinearity, J. Math. Anal. Appl., J. King Saud Univ. Sci. (multiple reviews of the same paper are not considered)
- author of 6 reviews for proceedings papers
- author of 42 reviews for zbMATH and 34 reviews for MathSciNet.

Teaching experience:

- teaching several courses at UHK since 2013 (e.g. Mathematics 1, Mathematics 2: Functions of Several Variables, Differential Equations, Mathematics 3: Processing of Measurement Data, Mathematics for Physics 1, Mathematics for Physics 2, Seminar of Mathematical Physics 1, Seminar of Mathematical Physics 2, Additional Mathematics 2)
- I am the author of six study texts for the taught subjects
- two master students and two bachelor students successfully defended their theses, moreover, I was a consultant of one other master student
- currently I am supervising a bachelor student and a postdoc

Grants and awards:

- | | |
|----------------------|--|
| 2015 – 2017: | Junior project of the Czech Science Foundation (CSF)
“Spectral and resonance properties of quantum models”,
principal investigator |
| 2022 – present: | Standard project of the CSF,
“Asymptotic and spectral analysis of operators
in mathematical physics”, principal investigator |
| Jan 2011 – Jan 2012: | Standard project of the CSF,
“Quantum mechanics of guided particles”, team member |
| 2017 – 2019: | Standard project of the CSF,
“Mathematical-Physics Models of Novel Materials”,
team member |

Jun 2020 – Dec 2020: Standard project of the CSF,
“Singular spaces from special holonomy and foliations”,
team member

2016, 2017: Prizes of the rector of the University of Hradec Králové
for the publication results for the year 2016
and for the year 2017.

Language skills:

Czech: native speaker

English: advanced

German: intermediate

Portuguese: beginner

Other activities:

2003 to 2008: one of the organizers of the physics competition FYKOS

2006 to 2010: member of the Student Chamber of the Academic Senate
of the Faculty of Mathematics and Physics

2013 to 2017, 2019: main organizer of the competition Náboj Junior in Hradec
Králové

2017 to present: member of the Council of Schools of Higher Education

2019 to present: member of the Academic Senate of the University of Hradec
Králové

In Hradec Králové, 1. 2. 2023

Jiří Lipovský